Survival signal REG3α prevents crypt apoptosis to control Acute Gastrointestinal graft-versus-host disease

Dongchang Zhao, Yeung-Hyen Kim, Seihwan Jeong, Joel K. Greenson, Mohammed S. Chaudhry, Matthias Hoepting, Erik R. Anderson, Marcel R.M. van den Brink, Jonathan U. Peled, Antonio L.C. Gomes, Ann E. Slingerland, Michael J. Donovan, Andrew C. Harris, John E. Levine, Umut Ozbek, Lora V. Hooper, Thaddeus S. Stappenbeck, Aaron Ver Heul, Ta-Chiang Liu, Pavan Reddy, James L. M. Ferrara

Supplementary Data

Table of contents

Supplementary Table 1. Primer sequences for quantitative PCR and antibodies for flow cytometry

Primer	Forward	Reverse
Reg3g	5'-TTC CTG TCC TCC ATG ATC AAA-3'	5'-CAT CCA CCT CTG TTG GGT TC-3'
IL-22	5'-CAT GCA GGA GGT GGT ACC TT-3'	5'-CAG ACG CAA GCA TTT CTC AG-3'
Defa1	5'-CTA GTC CTA CTC TTT GCC CT-3'	5'-TTG CAG CCT CTT GAT CTA CA-3'
Defa2	5'-ACT GAG GAG CAG TCA GGT GAA-3'	5'-GCC AAT GGT CAT CTT GTC CT-3'
S100a8	5'-TGT CCT CAG TTT GTG CAG AAT ATA AA-3'	5'-TCA CCA TCG CAA GGA ACT CC-3'
S100a9	5'-GGT GGA AGC ACA GTT GGC A-3'	5'-GTG TCC AGG TCC TCC ATG ATG-3'
Gapdh	5'-AGG TCG GTG TGA ACG GAT TTG-3'	5'-TGT AGA CCA TGT AGT TGA GGT CA-3'

Antibody/Fluorochrome	Clone	Company	Dilution
CD4-PerCP-Cy5.5	RM4-5	BD Biosciences	1:200
CD8-APC-eF780	53-6.7	eBioscience	1:200
TCRbeta-PE-Cy7	H57-597	eBioscience	1:200
FoxP3-APC	FJK-163	eBioscience	1:200
IFNgamma-FITC	XMG1.2	BD Biosciences	1:200
IL-10-PE	JES5-16E3	eBioscience	1:200
IL-17A-APC	eBio17B7	eBioscience	1:200
FC-blocker-CD16/32	2.4G2	BD Biosciences	1:400
CD24-PE-Cy7	M1/69	eBioscience	1:400
CD45-PE	30-F11	BD Biosciences	1:400
CD31-PE	390	eBioscience	1:400
TER-119-PE	TER-119	BD Biosciences	1:400
EpCAM-APC	G8.8	eBioscience	1:1000
Annexin V-Pacific Blue	N/A	eBioscience	1:20
DAPI (10μg/ml)	N/A	Sigma-Aldrich	1:600
7-AAD	N/A	eBioscience	1:20
Live/Dead viability dye/Violet	N/A	Molecular probes	1:1000

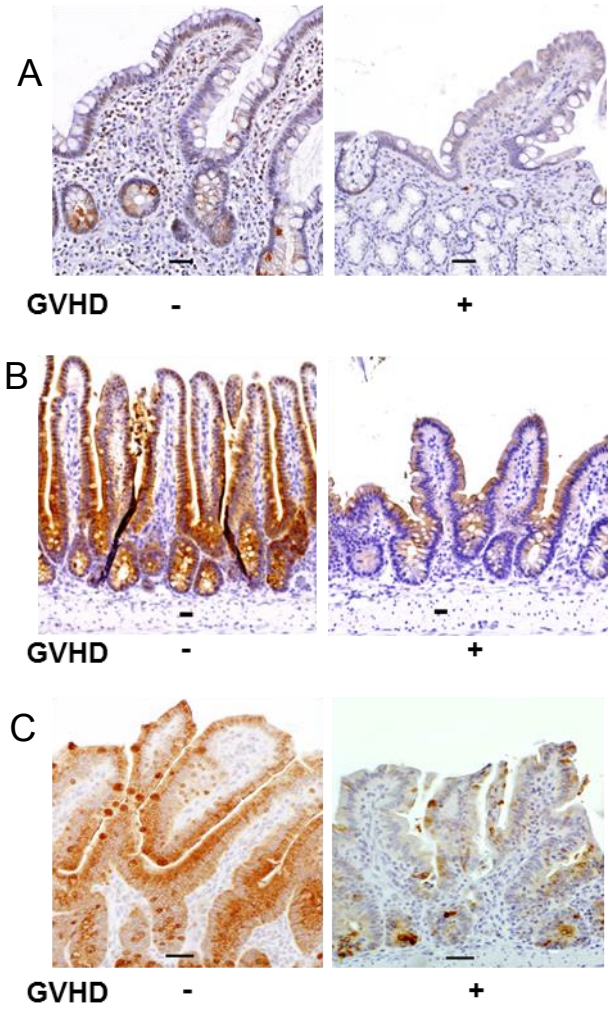

Supplementary Figure 1. REG3α/γ protein expression by immunohistochemistry. (A) REG3α protein expression in duodenal biopsies from individual patients summarized in Figure 1A-C. **(B)** REG3γ protein expression in the ileum sections from individual mice summarized in Figure 1D-F**.** (**C)** REG3γ protein expression in the ileum sections from individual mice summarized in Figure 1G-I**.** Images were taken with either an Olympus BX51 with a 40x objective **(A,C)** or an EVOS XL Core Imaging System from Life Technologies with a 20x objective **(B)**. Scale bars are 50 µm.

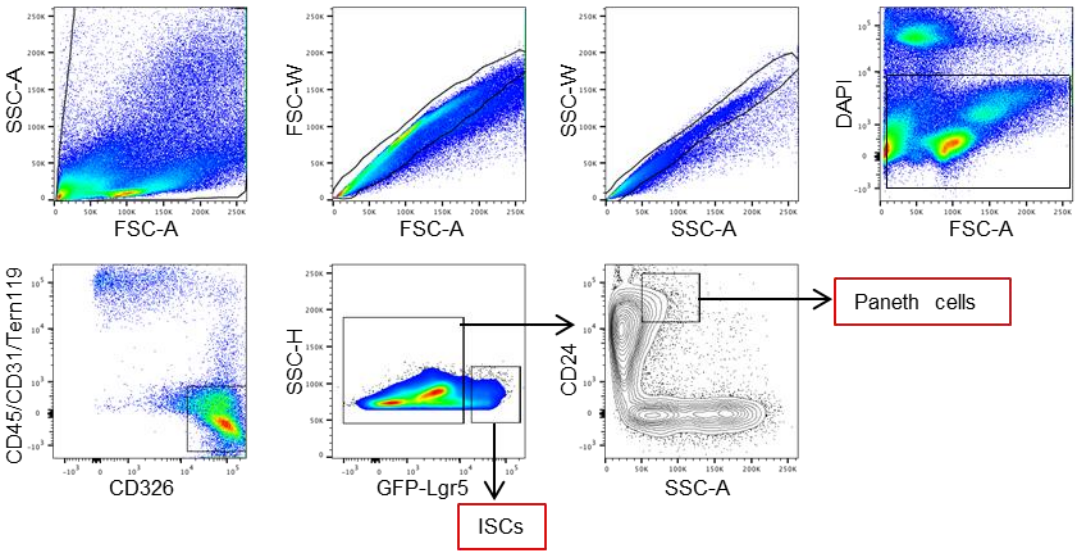

Supplementary Figure 2. Strategy analysis of Paneth cells and ISCs by flow cytometry. Small intestine crypt cells from Lgr5-EGFP^{+}-B6 mice were isolated and were identified as EpCAM^{+}CD45^{-}CD31^{-}TER-119^{-}DAPI^{-} cells. Within this compartment, Lgr5^{hi} were identified as ISCs. After excluding ISCs, Paneth cells were subsequently identified as CD24^{hi}Sidescatter^{hi} cells.

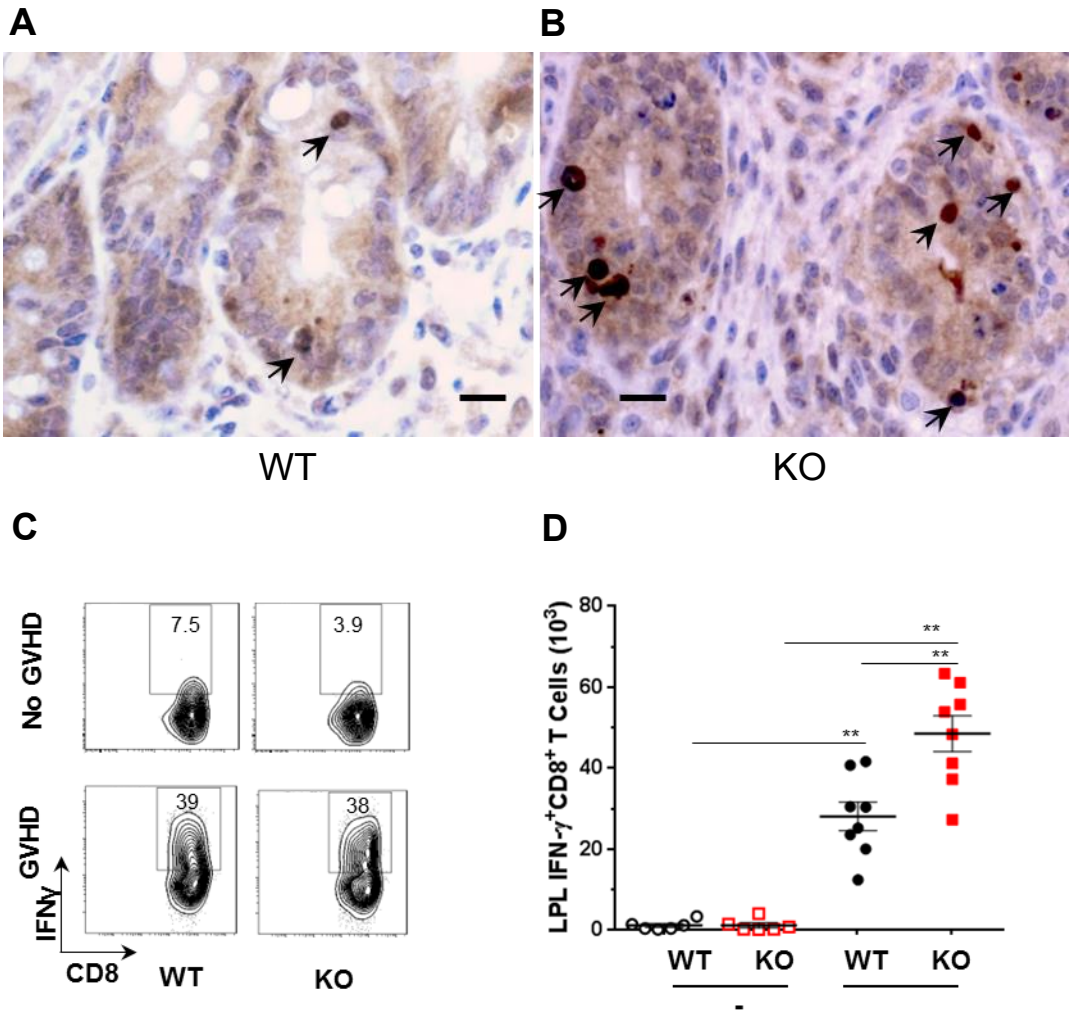

Supplementary Figure 3. Cleaved Caspase-3 staining and flow cytometric analysis of LPL IFNγ$^+$ T cells. (A,B) Cleaved Caspase-3 staining by immunohistochemistry in ileum from individual allogeneic **(A)** Wild type B6 (WT) or **(B)** B6-*Reg3g*$^{-/-}$ (KO) recipients with GVHD as summarized in Figure 4F. Images were taken with Zeiss AxioPlan2 with a 40x objective. Scale bars are 50 µm. **(C,D)** Wild type B6 (WT) and B6-*Reg3g*$^{-/-}$ (KO) mice underwent BMT from B6-Ly5.1 donors (GVHD −) or C3H.SW donors (GVHD +). Mice were euthanized on day +7 after BMT. T cells from isolated small intestine lamina propria lymphocytes (LPLs) were identified by flow cytometry as viable TCRβ$^+$ cells. CD8$^+$ IFNγ$^+$ T cells were subsequently **(C)** identified and **(D)** quantified from syngeneic recipients (GVHD −: WT ○, n=6; KO □, n=6) and allogeneic recipients (GVHD +: WT ●, n=8; KO ■, n=8). *P<0.05, **P<0.01, one-way analysis of variance (ANOVA). Data are expressed as mean ±SEM.

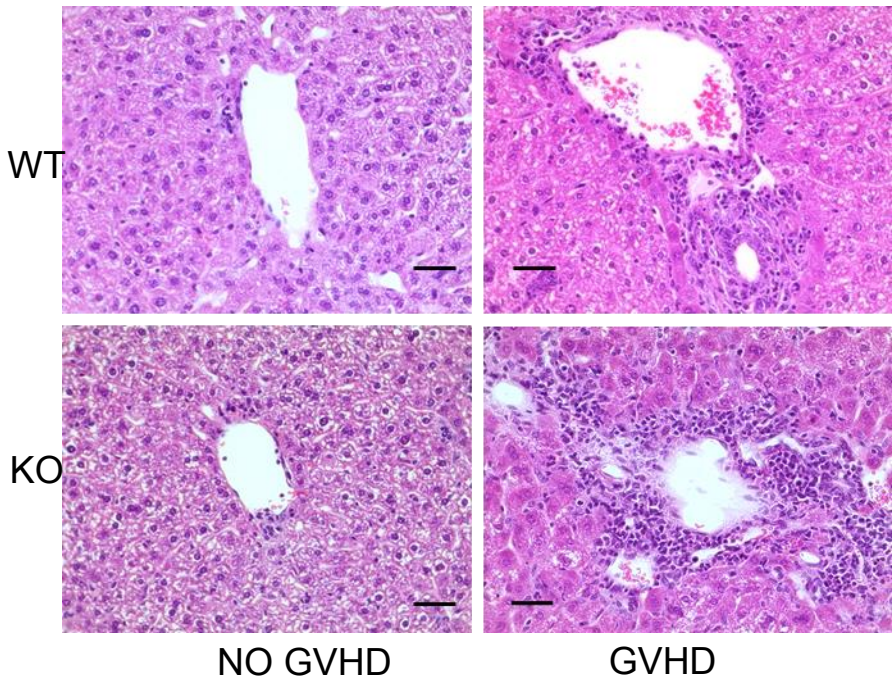

Supplementary Figure 4. Liver Histology in mice following BMT. Liver sections were stained with hematoxylin and eosin following harvest from individual mice analyzed in Supplementary Fig 3. Images were taken with EVOS XL Core Imaging System from Life Technologies with a 40x objective.

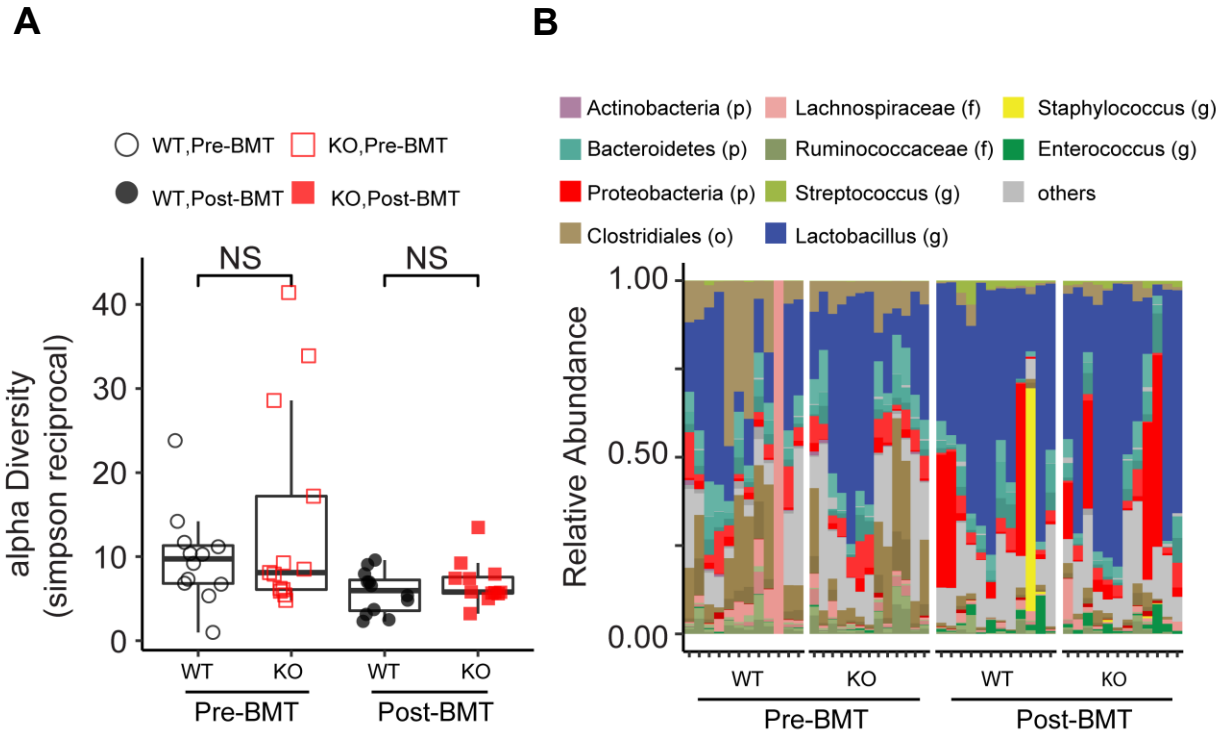

Supplementary Figure 5. Microbiota composition among wild type B6 (WT) and B6-*Reg3g*$^{-/-}$ (KO) mice. After co-housing for two weeks, wild type B6 (WT) and B6-*Reg3g*$^{-/-}$ mice underwent BMT from C3H.SW donors as described in Methods. Fecal samples of microbiota analysis were collected on one day before BMT (Pre-BMT) and day +7 after BMT (Post-BMT). **(A)** The alpha diversity of microbiota in WT (○, n=12) and KO (□, n=13) both at pre-BMT and post-BMT (WT ●, n=12; KO ■, n=13). NS= P>0.05, Wilcox test. **(B)** Microbiota composition per sample is displayed according to the relative abundance of relevant taxonomic groups, following the color-coding taxonomic scheme in the yingtools2 R package (https://github.com/ying14/yingtools2). p, phylum; o, order; f, family; g. genus.

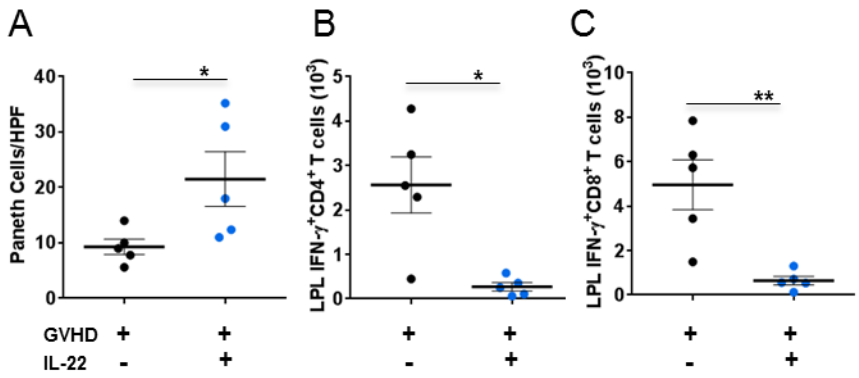

Supplementary Figure 6. Prophylactic administration of IL-22 reduces GVHD. B6D2F1 mice underwent BMT from allogeneic B6 donors (GVHD +), and were given PBS or IL-22 from day +1 (PBS ●, n=5; IL-22 ●, n=5). Samples were analyzed on day +7 after BMT. (**A**) Average Paneth cell numbers per high power field (HPF) in ileal tissue. (**B, C**) Quantification of LPL IFNγ$^+$ CD4$^+$ and CD8$^+$ T cells in the ileum by flow cytometry. *P<0.05, **P<0.01, unpaired two-tailed *t* test. Data are expressed as mean ±SEM.

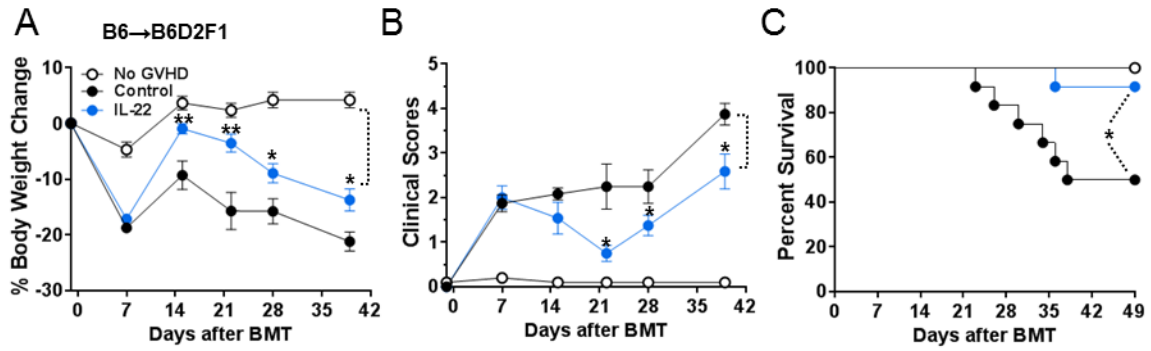

Supplementary Figure 7. IL-22 administration reverses the established clinical GVHD. (**A**) Serial body weight measurement, (**B**) GVHD clinical score analysis, and (**C**) survival of B6D2F1 mice after BMT from allogeneic B6 donors, treated with PBS (Control ●, n=12) or IL-22 (IL-22 ●, n=12) from day +7. As a no GVHD control, mice received BM only from the same donor strain (No GVHD ○, n=5). *P<0.05, **P<0.01. Data are expressed as mean ±SEM. unpaired two-tailed *t* test (**A,B**). *P<0.05, log-rank test (**C**).

.

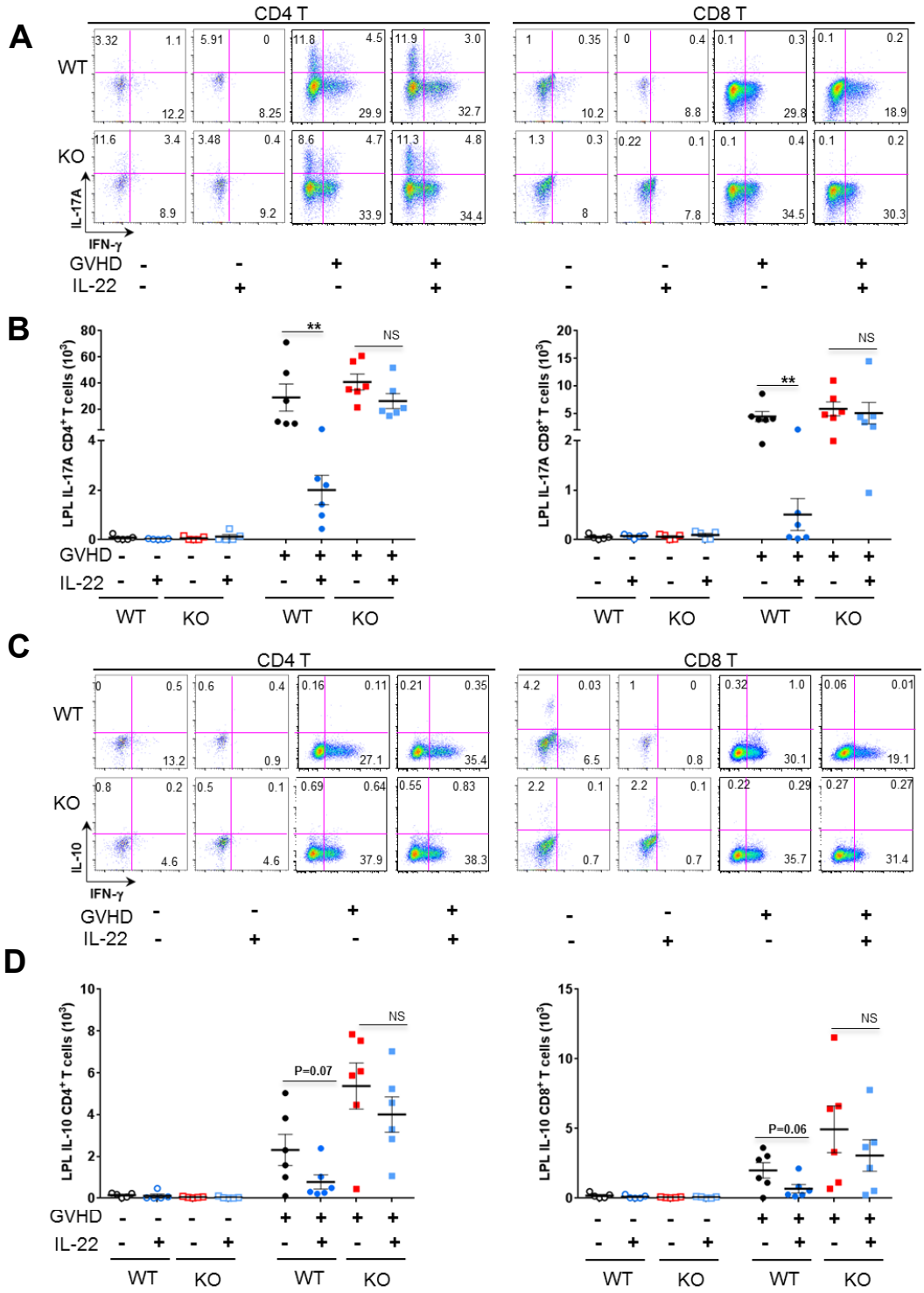

Supplementary Figure 8. Flow cytometric quantification of LPL IL-17$^+$ and IL-10$^+$ T cells. Wild type B6 (WT) and B6-*Reg3g*$^{-/-}$ (KO) mice received PBS or IL-22 injections from day +1 after BMT from B6-Ly5.1 donors (GVHD −: WT PBS ○, n=5; WT IL-22 ○, n=5; KO PBS □, n=5; KO IL-22 □, n=5) or C3H.SW donors (GVHD +: WT PBS ●, n=6; WT IL-22 ●, n=6; KO PBS ■, n=6; KO IL-22 ■, n=6). Small intestine was analyzed on day +7 after BMT. T cells from isolated LPLs were identified by flow cytometry as viable TCRβ$^+$ cells, and CD4$^+$ and CD8$^+$ subsets were analyzed. **(A)** Identification and **(B)** quantification of LPL CD4$^+$ and CD8$^+$ IL-17$^+$ cells. (**C**) Identification and (**D**) quantification of LPL CD4$^+$ and CD8$^+$ IL-10$^+$ cells. NS=P>0.05, *P<0.05, **P<0.01, unpaired two-tailed *t* test. Data are expressed as mean ±SEM.

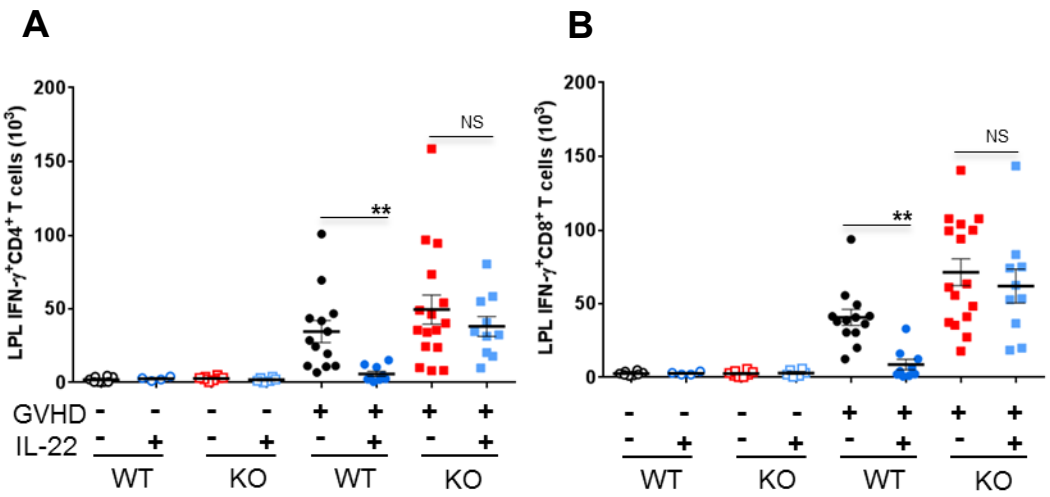

Supplementary Figure 9. Flow cytometric quantification of LPL IFNγ$^+$ T cells. Wild typeB6 (WT) and B6-*Reg3g*$^{-/-}$ (KO) mice received PBS or IL-22 injections from day +1after BMT from B6-Ly5.1 donors (GVHD −: WT PBS ○, n=8; WT IL-22○, n=4; KO PBS □, n=8; KO IL-22 □, n=6) or C3H.SW donors (GVHD +: WT PBS●, n=13; WT IL-22 ●, n=9; KO PBS ■, n=16; KO IL-22 ■, n=10). Small intestine was analyzed on day +7 after BMT for quantification of **(A)** CD4$^+$ and **(B)** CD8$^+$ LPL IFNγ$^+$ T cells as in Supplementary Fig. 8. NS=P>0.05, **P<0.01, unpaired two-tailed *t* test. Data are expressed as mean ±SEM.

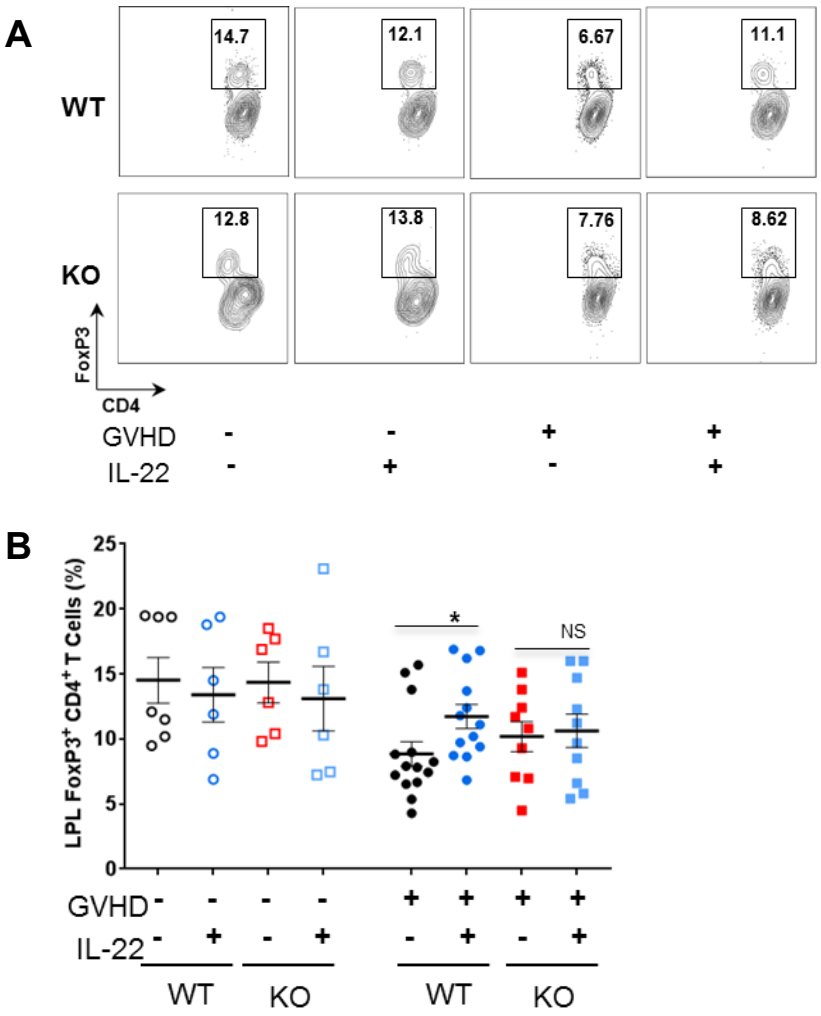

Supplementary Figure 10. Flow cytometric quantification of LPL Tregs. Wild type B6 (WT) and B6-*Reg3g*$^{-/-}$ (KO) mice received PBS or IL-22 injections from day +1 after BMT from B6-Ly5.1 donors (GVHD −: WT PBS ○, n=7; WT IL-22 ○, n=6; KO PBS □, n=6; KO IL-22 □, n=6) or C3H.SW donors (GVHD +: WT PBS ●, n=14; WT IL-22 ●, n=13; KO PBS ■, n=9; KO IL-22 ■, n=10). Small intestine was analyzed on day +7 after BMT as in Supplementary Fig. 8. (**A**) Isolated LPLs were identified by flow cytometry as viable TCRβ^{+} cells, and Tregs were subsequently identified as FoxP3^{+}CD4^{+} cells. (**B**) Quantification of LPL FoxP3^{+}CD4^{+} Treg cell, as a percentage of total CD4^{+} T cells. NS=P>0.05, *P<0.05, unpaired two-tailed *t* test. Data are expressed as mean ±SEM.

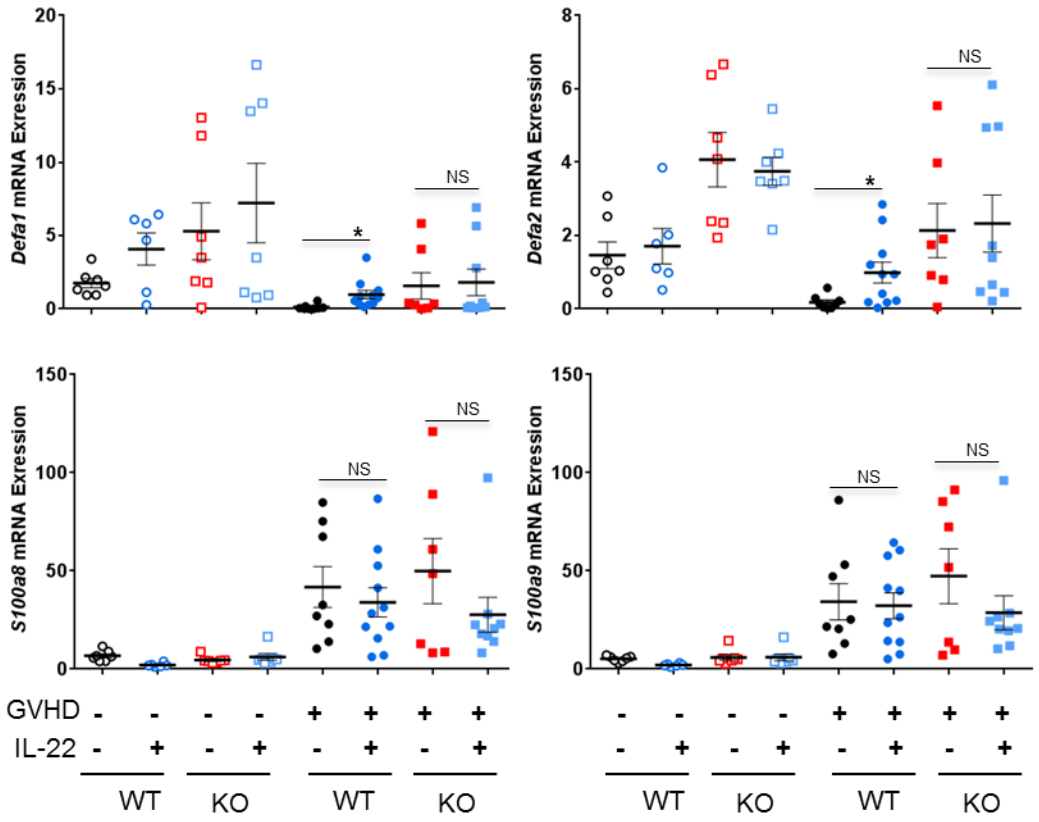

Supplementary Figure 11. Anti-microbial gene expression in the small intestine. Wild type B6 (WT) and B6-*Reg3g*$^{-/-}$ (KO) mice received PBS or IL-22 injections from day +1 after BMT from B6-Ly5.1 donors (GVHD −: WT PBS ○, n=7; WT IL-22 ○, n=6; KO PBS □, n=7; KO IL-22 □, n=7) or C3H.SW donors (GVHD +: WT PBS ●, n=8; WT IL-22 ●, n=11; KO PBS ■, n=7; KO IL-22 ■, n=9). Small intestine was analyzed on day +7 after BMT as in Supplementary Fig. 8. The genes of *Defa1*, *Defa2*, *S100a8* and *S100a9* mRNA expression were measured by qPCR. NS=P>0.05, *P<0.05, **P<0.01, unpaired two-tailed *t* test. Data are expressed as mean ±SEM.

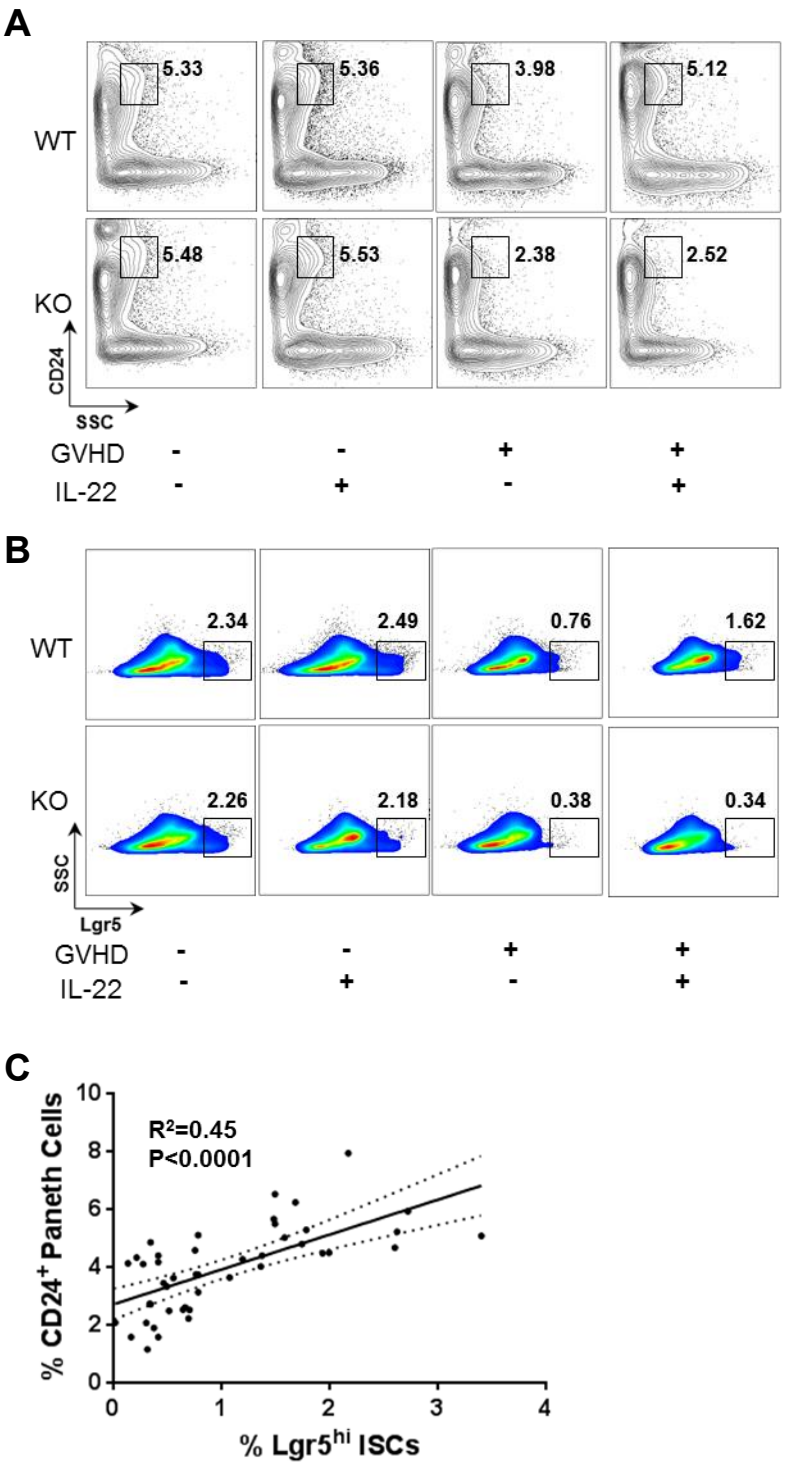

Supplementary Figure 12. Flow cytometric quantification of ISCs and Paneth cells. Wild type B6 (WT) and B6-*Reg3g*$^{-/-}$ (KO) mice (Lgr5-EGFP^{+}) received PBS or IL-22 injections from day +1 after BMT from B6-Ly5.1 donors (GVHD −) or C3H.SW donors (GVHD +). Small intestine was analyzed on day +7 after BMT. The gating strategy of ISC and Paneth cell was performed as in Supplementary Fig. 2. Identification of **(A)** Paneth cells and **(B)** ISCs as summarized in Figures 7 and 8. **(C)** Correlation of ISC and Paneth cell numbers in all mice treated with PBS as shown in Figures 7 and 8 (n=45), as calculated by the Pearson correlation coefficient.

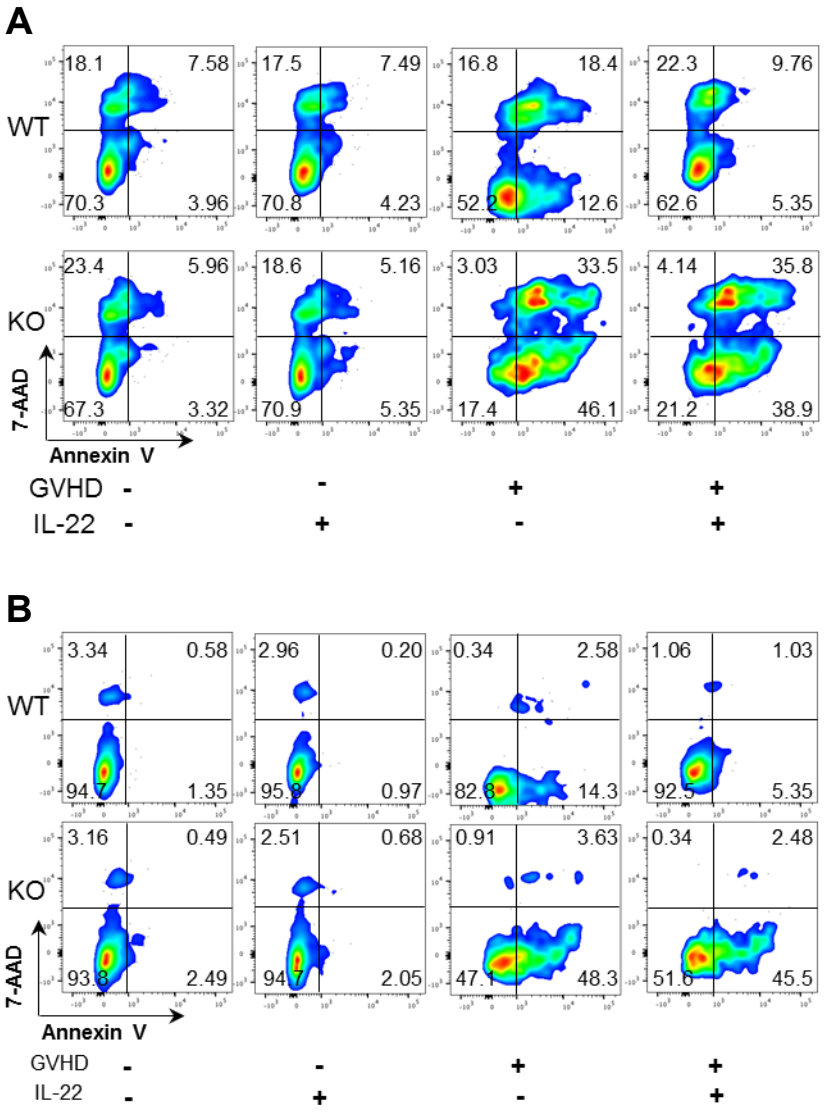

Supplementary Figure 13. Flow cytometric identification of Annexin V$^+$ apoptotic ISCs and Paneth Cells. Wild type B6 (WT) and B6-*Reg3g*$^{-/-}$ (KO) mice (Lgr5-EGFP$^+$) received PBS or IL-22 injections from day +1 after BMT from B6-Ly5.1 donors (GVHD −) or C3H.SW donors (GVHD +). Small intestine was analyzed on day +7 after BMT. The gating strategy of ISC and Paneth cell was performed as in Supplementary Fig. 2. Early apoptosis, defined as 7-AAD$^-$ Annexin V$^+$ in **(A)** Paneth cells and **(B)** ISCs from individual mice summarized in Figure **7** and 8.

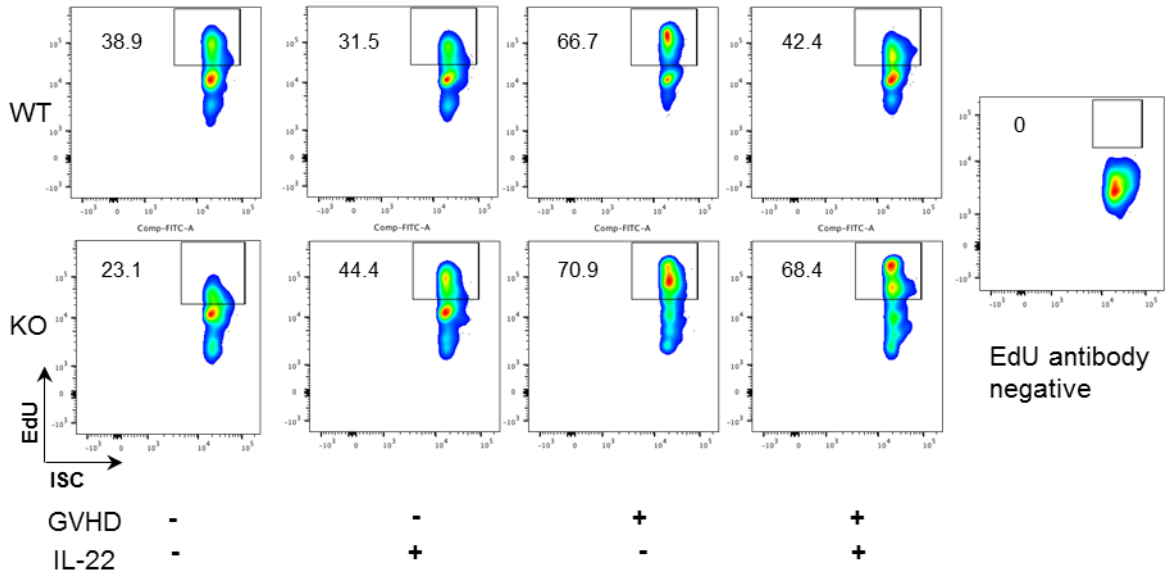

Supplementary Figure 14. Flow cytometric quantification of ISCs proliferation. Wild type B6 (WT) and B6-*Reg3g*$^{-/-}$ (KO) mice (Lgr5-EGFP^{+}) received PBS or IL-22 injections from day +1 to day +6 after BMT from B6-Ly5.1 donors (GVHD −) or C3H.SW donors (GVHD +). Mice were injected intraperitoneally with 200μL of 5mM EdU solution (Invitrogen) in PBS 2h before sacrifice. Small intestine was collected for EdU staining in ISCs. The gating strategy of ISC was performed as in Supplementary Fig. 2. Identification of EdU^{+} of ISCs as summarized in Figures 8.

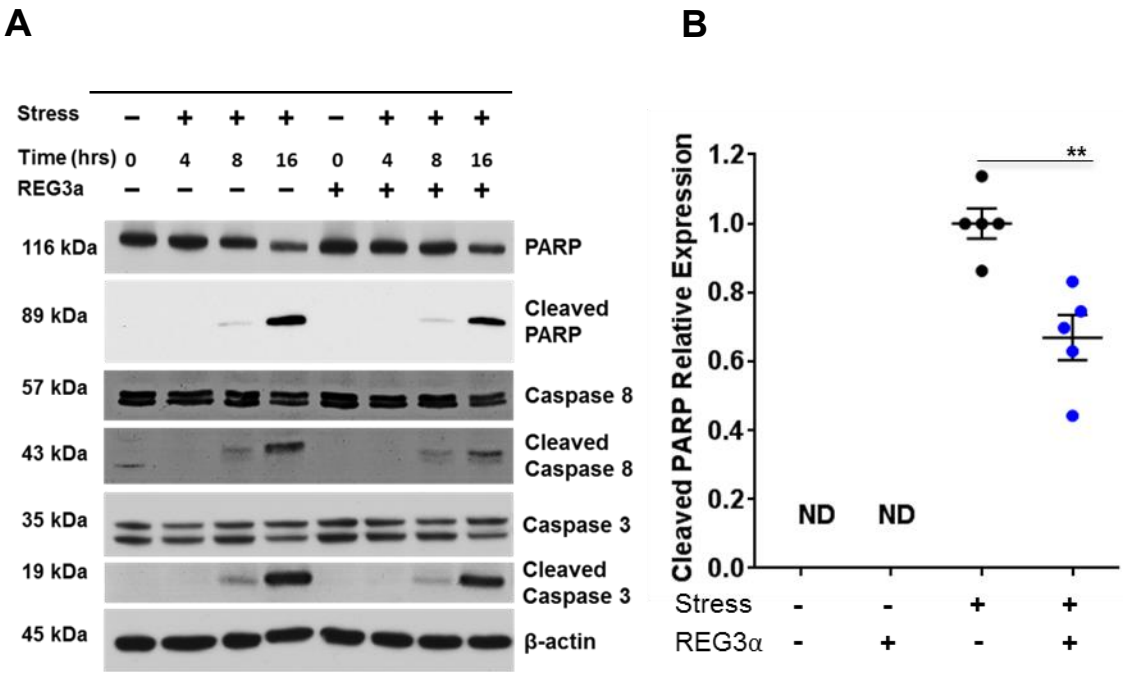

Supplementary Figure 15. REG3α prevented apoptosis of human intestinal epithelial cell lines in vitro. HT-29 cells were treated with human recombinant REG3α protein following apoptotic stimuli (stress) for 0, 4, 8 and 16 hours described in Methods. Cells lysates were collected for western blot analysis. **(A)** Immunoblots of PARP, cleaved PARP, Caspase-8, cleaved Caspase-8, Caspase-3, cleaved Caspase-3 and β-actin. **(B)** Quantification of cleaved PARP expression by western blot after 16 hours of cell culture. ND= not detectable, **P<0.01, unpaired two-tailed *t* test. Data are expressed as mean ±SEM.